Available online at www.sciencedirect.com

ScienceDirect

Procedia Structural Integrity 17 (2019) 198–205

Structural Integrity Procedia

www.elsevier.com/locate/procedia

ICSI 2019 The 3rd International Conference on Structural Integrity

Mean stress effect and fatigue crack closure in material from old bridge erected in the late 19th century

Grzegorz Lesiuk[a]*, Stephane Sire[b], Muriel Ragueneau[c], J.A.F.O. Correia[d], Bruno A.S. Pedrosa[e], A.M.P. De Jesus[d]

[a]*Faculty of Mechanical Engineering, Department of Mechanics, Materials Science and Engineering, Wrocław University of Science and Technology, Smoluchowskiego 25, 50-370 Wrocław, Poland*
[b]*University of Brest, IRDL, UMR CNRS 6027, 29200 Brest, France*
[c]*SNCF Réseau, DGII-OA, 93210 La Plaine Saint-Denis, France*
[d] *INEGI/Faculty of Engineering, University of Porto, Rua Dr. Roberto Frias, 4200-465 Porto, Portugal*
[e]*ISISE, Department of Civil Engineering, University of Coimbra, Rua Luís Reis Santos, Pólo II, 3030-788 Coimbra, Portugal.*

Abstract

The problem considered in this paper is the structural integrity of old materials from the 19th century by means of fatigue crack growth problem. The authors present an overview of the fatigue fracture properties of old puddle iron members extracted from long-term operated bridges located in France. The fracture properties and fatigue crack growth results for 19th-century puddle iron are presented and compared with typical Kinetic Fatigue Fracture Diagram (KFFD) constructing methods. The presented results for fatigue crack growth rate description under mode I using $\Delta K_{applied}$ approach and $\Delta K_{effective}$ approach differs significantly using variable mean stress effect – R-ratio (0.05; 0.7). As it was demonstrated, the hysteresis loop analyses allow to obtain the estimated crack closure level. From the engineering point of view, there is a strong need for generalization of the KFFDs description using mean stress robust parameter involving local crack tip behavior for old puddle iron. Additionally, there are discussed the strengthening methods based on CFRP for this type of ancient materials in the light of the obtained numerical results for strengthened and non-strengthened puddle iron/steel specimens using CFRP patches using local approach.

Peer-review under responsibility of the ICSI 2019 organizers.

Keywords: puddle iron, fatigue crack growth, lifetime predictions, fracture analysis

* Corresponding author. Tel.: +48 713203919; fax: +48 713211235.
E-mail address: Grzegorz.Lesiuk@pwr.edu.pl

2452-3216
Peer-review under responsibility of the ICSI 2019 organizers.
10.1016/j.prostr.2019.08.027

1. Introduction

Fatigue and fracture are one of the most frequent causes of machine or construction failures. On that canvas, an application of CFRP patches to reinforce long-term operated structures made of steel, evaluated in fatigue crack growth context, seems to be a rational way to extend their service life and, hence, its further safe exploitation. Especially, this issue is vivid for stemming from 19th and the beginning of 20th-century bridges which were usually built of components made of a puddle or mild iron. One of the most important parts of engineering analysis is the estimation of fatigue crack growth rate (Lesiuk et al. 2019; Kotowski et al. 2018; Correia et al. 2017; Jesus et al 2011). In several approaches (Zhu et al., 2017), (Lesiuk et al., 2017), (Correia J.A.F.O. et al., 2016) the mean stress effect plays an important role in fatigue analysis. Therefore the R-ratio avoidance is still a vital topic. According to the origin Elber work (Elber, 1970), the crack closure phenomenon seems to be particularly worth for analysis and implementation in the light of the material limitations (and experimental trials) of long term operated 19th-century structures using ΔK effective approach. Several laws have been proposed to take into account the crack closure effects on the materials when subjected to fatigue crack propagation and can be seen in (Correia et al., 2016). Based on the above, the fracture mechanics allows for effective and relatively sufficient estimation of subcritical fatigue growth period of pure metal alloy components without any reinforcement. Below, is presented a part of the experimental campaign and numerical analysis of the fatigue fracture mechanics approach necessary for further calculation of material behaviour in real structures including SIFs for various reinforcements of long term operated steel components.

2. Microstructure and chemical composition of the metallic material

The object of investigation was material extracted from 19th-century old bridge. This structure, located in Bayonne (Pyrénées-Atlantiques department in France) was built between 1862 and 1864 and was over the Adour River. This bridge was demolished in May 2013 and replaced by a modern one. Made of puddled iron, it was composed of five spans (46.64 m + 3×59.52 m + 46.64 m) for a total length of approximately 272m. The main girders were 5.50 m high and included St. Andrews cross trusses, which is a characteristic of metal constructions during the second half of the 19th century. The floor beams had a span of 14.56 m and a height of 2.50 m; stringers were 500 mm high.

Based on their quality of preservation, iron parts were chosen and recovered during the demolition of the bridge. The methodology used for the choice of these elements and the description of the bridge is presented in (Gallegos Mayorga et al., 2017). The plate used for this study is 12mm thick and the composition of the iron is presented in the following Table 1.

Table 1. Chemical composition (in % by weight) of tested puddle iron compared with typical puddle irons and old mild steels.

Materials	C	Mn	Si	P	S
investigated puddle iron	<0.01	<0.02	0.28±0.02	0.41±0.02	0.054±0.04
typical values for puddle irons	<0.8	0.4	n/a	<0.6	<0.04
typical values for old mild steels	<0.15	0.2÷0.5	Variable	<0.06	<0.15

The noticeable feature of each puddle iron is a fact of high phosphorus content and numerous of non-metallic inclusions reflected in metallographic observations. The microstructure of tested puddle iron is shown in Fig. 1. A typical microstructure of puddle iron is mostly shaped by numerous of non-metallic inclusions and different ferrite grain size (Lesiuk et al. 2019; Krechkovska et al. 2018). Enlarged ferrite grains structure is shown in Fig. 1 (on the right).

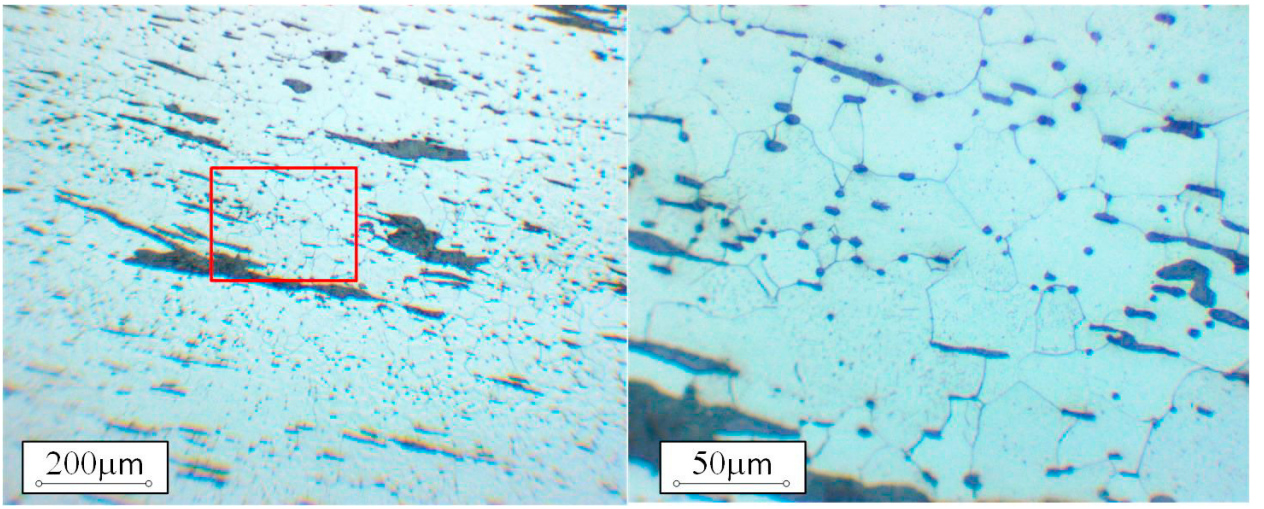

Fig. 1. The microstructure of tested puddle iron from Bayonne

3. Fatigue Crack growth test results

Fatigue crack growth rate experiment was performed in accordance with ASTM E647 standard (ASTM, 2015). For the experiment, CT specimens were designed (W=50mm, B=8.5 mm). Notch was machined using EDM (electro discharging machine) with root radius 0.2 mm. The initial normalized crack length was equal to 0.2. Initially, the precracking procedure was involved using ΔK-controlled test does not exceed 15 MPa·m$^{0.5}$. The test started from an initial value of ΔK in order to avoid the plastic zone influence created during the precracking procedure. Experiments were performed for two different mean stress level characterized by the stress R-ratio equal to 0.05 and 0.7, with sinusoidal-shaped loading waveform (test frequency f=10 Hz). Quantity of crack length was monitored using ASTM E647 compliance method. During the experiment, the signals of force F, displacement u and crack opening displacement (COD measured in load line) were collected. For each chosen cycle, at least two hysteresis loops were registered in order to assess the F-COD behaviour during the test in order to evaluate crack closure parameters: F_{cl} and K_{cl}. The main idea of obtaining F_{cl} consists of the splitting recorded F-COD curve into two curves. First of them is linear (described by Eq. 1) and second is nonlinear (described by Eq.2). Simplified approach considering the nonlinear part as quadratic one is shown in Figure 2.

$$\hat{v}_L(F) = A_0 + A_1 F \tag{1}$$

$$\hat{v}_Q(F) = B_0 + B_1 F + B_2 F^2 \tag{2}$$

Where
$\hat{v}_L(F)$ – the linear function of a linear regime of the recorded hysteresis loop,
$\hat{v}_Q(F)$ – the quadratic function of a non-linear regime of the recorded hysteresis loop.

From linear regression, the constants A_0 and A_1 can be easily estimated. However, the constants B_0, B_1, B_2 are unknown and they should respect the following conditions from the common F_k – "knee" value identification:

$$\hat{v}_Q(F) = \hat{v}_L(F) \tag{3}$$

$$\frac{d(\hat{v}_Q(F))}{dF} = \frac{d(\hat{v}_L(F))}{dF}\hat{v}_L(F) \text{ (for } F=F_k\text{)} \tag{4}$$

According to the above conditions, we obtain:

$$\begin{aligned} B_1 + 2B_2F_k &= A_0 + A_1F_k \\ B_0 + B_1F_k + B_2F_k^2 &= A_0 + A_1F_k \end{aligned} \tag{5}$$

The constants B_0, B_1, B_2 should be optimal from the mathematical point of view. In order to obtain their optimal values, we can find the mentioned constants by minimalizing the residual sum of squares ξ (RSS) defined as:

$$\xi = \frac{1}{(COD_{\max} - COD_{\min})^2} \cdot \sum_{i=1}^{N} \begin{Bmatrix} (\hat{v}_Q(F_i) - v_i)^2 \text{ for } P_i < P_k \\ (\hat{v}_L(F_i) - v_i)^2 \text{ for } P_i \geq P_k \end{Bmatrix}. \tag{6}$$

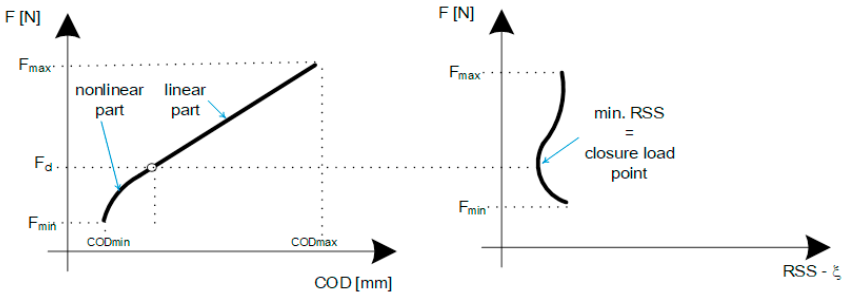

Fig. 2. The schematic idea of the closure load estimation

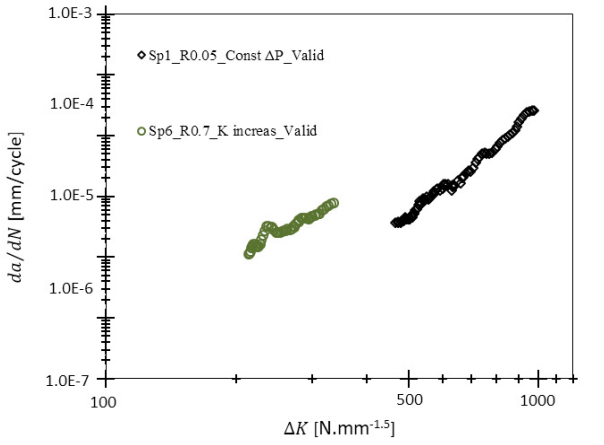

Fig. 3. ΔK-kinetic fatigue fracture diagram for tested puddle iron

Fig. 3 represents typical ASTM E647 da/dN-ΔK kinetic fatigue fracture diagram. As it is noticed (and expected) the contribution of R-ratio significantly affects the fatigue crack growth rate data.

On the other hand, Fig. 4. represents crack-closure da/dN-ΔK_{eff} kinetic fatigue fracture diagram. In this case, the mean stress effect is strongly reduced.

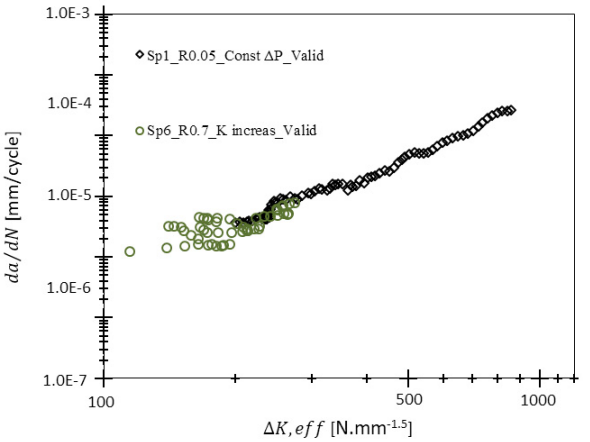

Fig. 4. ΔK_{eff}-based kinetic fatigue fracture diagram for tested puddle iron

Fracture surface analysis was performed using SEM (Scanning Electron Microscope). Fig. 5 presents the fatigue fracture surface of the specimen (R=0.05) after FCGR (fatigue crack growth rate) test. Enlarged (Fig. 5 – right side) area of the initial (ΔK approx. 15MPa·m) fatigue crack path is characterized by brittle facets of fatigue crack growth with multi-origin fatigue cracks caused by a large number of non-metallic inclusions. Typical – final fracture surface for high ΔK – is presented in Fig. 6. The main dominant mechanism is also caused by brittle fatigue fracture facets (marked by red frame) with typical regions for fatigue fracture. As previously, the fracture pattern is shaped by non-metallic inclusion with secondary cracks.

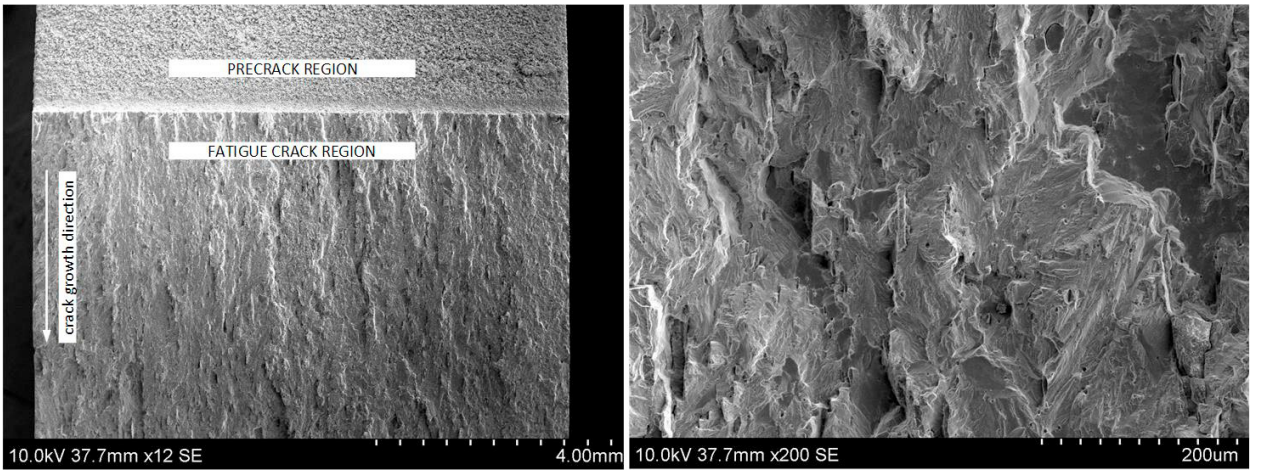

Fig. 5. The initial fatigue fracture surface of the tested specimen R=0.05; macro-view (on the left), enlarged fracture area (on the right)

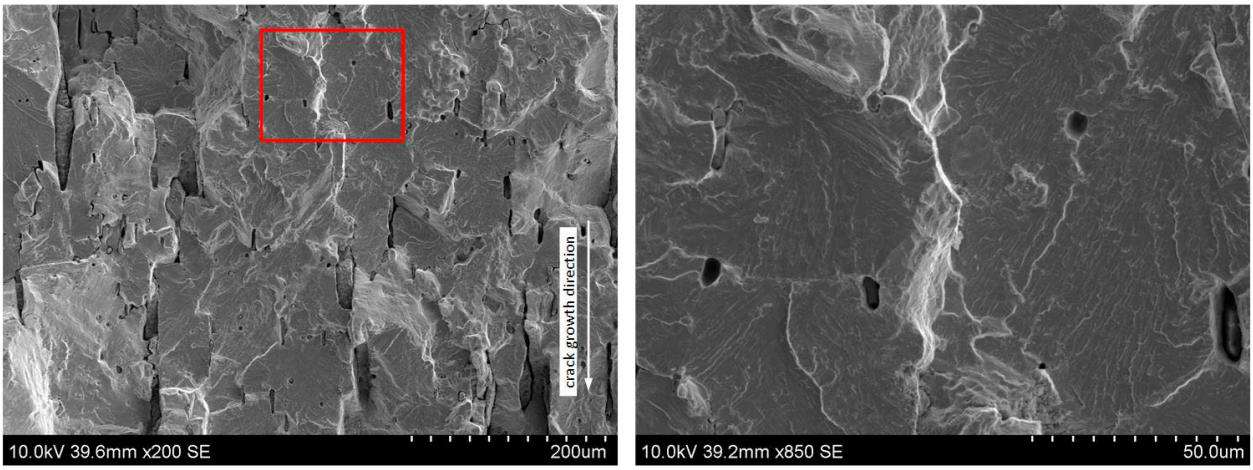

Fig. 6. The final stage of the fracture surface of the tested specimen R=0.05; macro-view (on the left), enlarged fracture area marked by frame (on the right)

4. Numerical analysis of strengthening efficiency

Previous work related to numerical analysis of strengthened cracked steel specimens was developed by Lesiuk et al. (2017) with the aim of obtaining the reduced stress intensity factor (SIF). Dekker et al. (2019) developed a cohesive xFEM model for simulating fatigue crack growth under mixed-mode loading. In this way,numerical investigations were performed in order to determine stress intensity factors (SIF) for strengthened and non-strengthened CT specimens. FE (Finite Element) analyses were performed with 3D models using ABAQUS® software (Abaqus, 2012). The geometry of the specimen follows the recommendations on ASTM E647 using W (main dimension) equal to 50 mm and B (thickness) equal to 8 mm. Numerical models are presented in Figure 7. Two types of strengthening solutions were studied with CFRP patches with 1.4 mm thickness: full face patch (wide equal to 31 mm) – see Figure 7 a) – and two patches (each patch with wide equal to 10 mm) – see Figure a b). Both solutions have CFRP patches with the edge at equal to 19 mm (initial crack length).

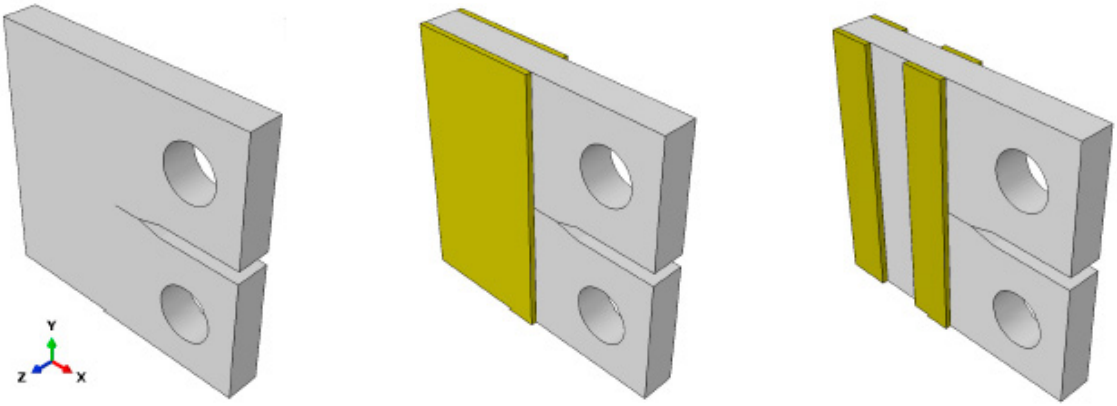

a) b) c)

Fig. 7. Numerical models: a) Non-strengthened; b) Strengthened full face patch; c) Strengthened two patches.

Stress intensity factors were computed for different values of crack length: 19 mm, 24 mm, 29 mm and 34 mm. Boundary conditions were defined as Ux=Uy=Uz=0 (pinned) for one hole and as Ux=Uy=0 for the loaded hole. Load and boundary conditions were applied on reference points which were coupled by rigid links (Kinematic Coupling) to the hole surfaces. A force equal to 4900 N was applied in the direction for crack opening. The interaction between CT specimen and CFRP patches was modelled with a tie constraint which means that

translational and rotational motion are equal in both surfaces. For both puddle iron and CFRP parts, material properties were defined as linear elastic using the value of Young Modulus equal to 200 GPa in the case of puddle iron and 160 GPa in the case of CFRP. Finite elements were defined as 8-node brick elements with reduced integration C3D8R. The computation of SIF was performed using the Extended Finite Element Method (xFEM) which is an extension of the conventional finite element method based on the concept of partition of unit (Melenk, J.M. and Babuska, I., 1997; Dekker et al. 2019) allowing for local enrichment functions to be easily incorporated into a finite element approximation (Abaqus, 2012). SIF was extracted for the first 5 contours and for all nodes through the thickness. The final value for each case study was extracted from the 5th contour. For non-strengthened specimen, the final value of SIF was extracted from the node at the surface since it is near the surface where plane stress formulation is more evident (and not in the middle). For strengthened specimens, the final value of SIF was defined as the average value between all nodes through the thickness. The value of the load range, ΔF, is obtained with the maximum load (4900 N) and the stress ratio equal to 0.1. Analytical SIF were also computed using ASTM E647 recommendations in order to compare with the SIF obtained for the non-strengthened specimen. The numerical results of the analysis are included in Fig. 8 – compared with analytical solutions of stress intensity factor for CT specimen from ASTM E647 standard.

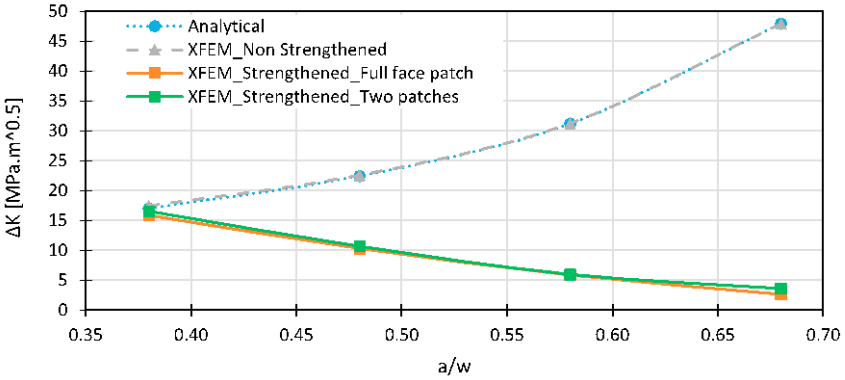

Fig.8. SIFs values for non-strengthened and strengthened specimens

It is observed, that both strengthening methodologies using CFRP patches contribute to reducing significantly the value of SIF, namely for longer crack lengths. When the crack is not in the zone covered by CFRP patches (a = 19 mm), the SIF reduction is low – which is clear from the physical point of view, but it increases significantly when the crack is longer. The difference between full face strengthening and two patches strengthening is not high. This study shows that using CFRP patches to improve the fatigue strength of materials can be a very good solution, however, further investigation is needed especially concerning the interface properties between CFRP patches and old material component.

5. Conclusions

Based on the performed experimental, fatigue fracture tests and numerical analysis, the following conclusions can be drawn:

- An old puddle iron (1864) was investigated under cyclic conditions with respect to the different mean stress level. Obtained results for tested puddle iron were affected by R-ratio effect.
- The fatigue crack closure measurements were performed using ΔK_{eff} approach. Using ΔK_{eff}, the mean stress effect can be neglected.
- The key point of future rehabilitation is prolonging the fatigue lifetime of cracked members. Using the CFRP patches, strengthening strategy can be suitable for old structural members (from puddle iron or old mild steel) with fatigue cracks.

- The main mechanism of fatigue crack growth retardation is associated with local ΔK decreasing and crack closure due to CFRP patches.
- Further experiments and numerical simulations are required in order to determine the optimal conditions of the CFRP patches (load state, fibre orientation etc.) in terms of local crack closure measurements.

Acknowledgements

This work was financially supported by the Wrocław University of Science and Technology grant no 0402/0084/18.

References

Abaqus (2012), Analysis User's Manual, Vol. 6, Dassault Systèmes, Hibbitt, Karlsson & Sorensen, Inc., Simulia, Providence, RI, p. 12.

A.M.P.D. Jesus, A.L.L.D. Silva, M.V. Figueiredo, J.A.F.O. Correia, A.S. Ribeiro, A.A. Fernandes, "Strain-life and crack propagation fatigue data from several Portuguese old metallic riveted bridges", Engineering Failure Analysis, vol. 18, no. 1, 2011, pp. 148-163.

Elber, W. Fatigue crack closure under cyclic tension. Eng. Fract. Mech. 1970, 2, 37–45.

G. Lesiuk, M. Szata, José A.F.O. Correia, A.M.P. De Jesus, P. Kucharski, Filippo Berto, "Kinetics of fatigue crack growth and crack closure effect in long term operating steel manufactured at the turn of the 19th and 20th centuries". Engineering Fracture Mechanics, Volume 185, 2017, Pages 160-174. {http://doi.org/10.1016/j.engfracmech.2017.04.044}

G. Lesiuk, J.A.F.O. Correia, M. Smolnicki, A.M.P. De Jesus, M. Duda, P.A. Montenegro, R.A.B. Calcada, "Fatigue crack growth rate of the long term operated puddle Iron from the Eiffel bridge", Metals, vol. 9, no. 1, 2019, Article number 53.

G. Lesiuk, M. Katkowski, J. Correia, A.M.P. de Jesus, W. Blazejewski, "Fatigue crack growth rate in CFRP reinforced constructional old steel", International Journal of Structural Integrity, vol. 9, no. 3, 2018, pp. 381-395.

G. Lesiuk, B. Rymsza, J. Rabiega, J.A.F.O. Correia, A.M.P. De Jesus, R. Calcada, "Influence of loading direction on the static and fatigue fracture properties of the long term operated metallic materials", Engineering Failure Analysis, vol. 96, 2019, pp. 409-425.

H. Krechkovska, O. Student, G. Lesiuk, J. Correia, "Features of the microstructural and mechanical degradation of long term operated mild steel", International Journal of Structural Integrity, vol. 9, no. 3, 2018, pp. 296-306.

J.A.F.O. Correia, A.M.P. De Jesus, P.M.G.P. Moreira, P.J.S. Tavares, "Crack Closure Effects on Fatigue Crack Propagation Rates: Application of a Proposed Theoretical Model", Advances in Materials Science and Engineering, vol. 2016, 2016, Article number 3026745.

José A.F.O. Correia, Sergio Blasón, Attilio Arcari, M. Muñiz-Calvente, Nicole Apetre, Pedro M.G.P. Moreira, Abílio M.P. De Jesus, Alfonso Fernández-Canteli, "Modified CCS fatigue crack growth model for the AA2019-T851 based on plasticity-induced crack closure". Theoretical and Applied Fracture Mechanics, Volume 85, Part A, October 2016, Pages 26–36. {http://dx.doi.org/10.1016/j.tafmec.2016.08.024}

J.A.F.O. Correia, A.M.P. De Jesus, R. Calçada, B. Pedrosa, C. Rebelo, L.S. Da Silva, G. Lesiuk, "Statistical analysis of fatigue crack propagation data of materials from ancient portuguese metallic bridges", Frattura ed Integrita Strutturale, vol. 11, no. 42, 2017, pp. 136-146.

L. Gallegos Mayorga, S. Sire, J.A.F.O. Correia, A.M.P. De Jesus, C. Rebelo, A. Fernández-Canteli, M. Ragueneau, B. Plu, "Statistical evaluation of fatigue strength of double shear riveted connections and crack growth rates of materials from old bridges", Engineering Fracture Mechanics, vol. 185, 2017, pp. 241-257.

L. Gallegos Mayorga, S. Sire, M. Ragueneau, B.Plu, "Understanding the behaviour of wrought-iron riveted assemblies: manufacture and testing in France", Proceedings of the Institution of Civil Engineers - Engineering History and Heritage, Volume 170, Issue 2 (2017), pp. 67-79

ASTM E647-15a - Standard Test Method for Measurement of Fatigue Crack Growth Rates (2015).

Melenk, J.M. and Babuska, I. (1997), "The Partition of Unity Finite Element Method: basic theory and application", International Journal for Numerical Method in Engineering, Vol. 40 No. 4, pp. 289-314.

P. Kotowski, G. Lesiuk, J.A.F.O. Correia, A.M.P. De Jesus, "Mixed mode (I+II) fatigue crack paths in S355J0 steel in terms of fractal geometry", AIP Conference Proceedings, vol. 2028, 2018, Article number 020005.

R. Dekker, F.P. van der Meer, J. Maljaars, L.J. Sluys, "A cohesive XFEM model for simulating fatigue crack growth under mixed-mode loading and overloading", International Journal for Numerical Methods in Engineering, vol. 118, no. 10, 2019, pp. 561-577.

S.P. Zhu, Q. Lei, Q.Y. Wang. Mean stress and ratcheting corrections in fatigue life prediction of metals. Fatigue & Fracture of Engineering Materials & Structures, 2017, 40(9): 1343-1354.